NUKLEONIKA 2004;49(Supplement 2):S61–S65

PROCEEDINGS

Alternative size and lifetime measurements for RHIC

Scott Pratt

Abstract Two-particle correlations based on the interference of identical particles have provided the chief means for determining the shape and lifetime of sources in relativistic heavy ion collisions (RHIC). Here, strong and Coulomb induced correlations are shown to provide similar information.

Key words correlations • interferometry • identical particles • heavy ion collision

S. Pratt
Department of Physics and Astronomy,
Michigan State University,
East Lansing Michigan, 48824, USA,
Tel.: 517 355 9200 x 2016, Fax: 517 353 4500,
e-mail: prattsc@msu.edu

Received: 12 December 2003, Accepted: 23 April 2004

In this workshop, we have seen remarkable evidence of the rapid progress of two-pion and two-kaon correlations with regards to determining the space-time characteristics of emitting sources in collisions from RHIC. These correlations are driven by the identical-particle interference of two bosons [10]. Over the last twenty years, the measurements and associated phenomenology have increased in their sophistication to the point where all six dimensions of the correlations are currently being exploited as can be seen in [17].

The results from two-pion correlations at RHIC [1, 2, 4] have shattered expectations [8, 21, 24, 25] of long-lived sources which should have resulted from the softening of the equation of state accompanying the deconfinement transition. Hydrodynamic calculations that incorporate lattice-gauge inspired equations of state and breakup criteria consistent with expected hadronic cross sections predict sources which stay together for times of 15–20 fm/c with continuous emission during the transverse expansion. Instead, two-pion correlations [17, 18] are consistent with sources which disassociate at ~10 fm/c in a sudden flash [6, 17]. Even more remarkably, the transverse size of the system appears to be near 13 fm, which would require an extremely rapid acceleration of the system which begins life with a transverse radius of ~6 fm. Although surface velocities indeed appear to be of the order of 0.7 c in blast-wave fits to spectra, that velocity must be attained in a very short time for the matter to reach 13 fm in 10 fm/c. Cascade calculations [11, 16], which do not include a softening to the equation of state, can fit the overall source size but under-predict the transverse dimension of the emitting source.

Without going into detail, the correlation function is principally determined by the particle separation distribution,

(1)

$$g(\mathbf{v},\mathbf{r}) = \frac{\int d^4x_a d^4x_b S_a(\mathbf{v},x_a) S_b(\mathbf{v},x_b) \delta^3\left(\mathbf{r} - \left[x_a - x_b - \mathbf{v}(t_a - t_b)\right]\right)}{\int d^4x_a d^4x_b S_a(\mathbf{v},x_a) S_b(\mathbf{v},x_b)}.$$

Here, S_a provides the probability of emitting a particle of velocity v at space-time coordinate x_a, and $g(\mathrm{v},\mathbf{r})$ gives the chance that two particles of the same velocity are separated by $\mathbf{r}$ on their asymptotic trajectories. Since the measured correlation function, $C(\mathbf{q},\mathbf{r})$, is itself a six-dimensional function, one can only extract three dimensions of space-time information about the source for any velocity v. Thus, time has to be extracted by assuming a symmetry between the spatial characteristics in the two transverse directions. The dimension of the $g(\mathrm{v},\mathbf{r})$ in the outwards (parallel to v) direction is then stretched if the source is long-lived, i.e.,

(2) $$R_{out}^2(\mathrm{v}) \approx R_\perp^2(\mathrm{v}) + \mathrm{v}^2\tau^2(\mathrm{v}), \quad R_{side} \approx R_\perp$$

where $R_\perp$ is the transverse spatial size of the source. Thus, the comparison of R_{out} to R_{side} provides information regarding the length of time over which emission occurs. In addition to the outwards and sidewards dimensions, the longitudinal dimension, R_{long}, also provides information about the temporal characteristics of the emission. The asymptotic probability cloud describing particles moving asymptotically with zero rapidity is confined to a fraction of the overall longitudinal extent of the source since high-rapidity sources are unlikely to emit particles with zero rapidity. If the distribution of sources are uniformly spread through all rapidity, and if the position of sources are described by a Bjorken (no longitudinal acceleration) expansion, $z = \mathrm{v}_{source}t$, the size of the probability cloud is determined by the velocity gradient,

(3) $$R_{long} = \frac{\mathrm{v}_{therm}}{d\mathrm{v}_z / dz} = \mathrm{v}_{therm}\tau.$$

Here, τ is the mean time at which breakup occurs. For transverse masses much larger than the temperature, $M_t \equiv \sqrt{M^2 + p_t^2} >> T$, the thermal velocity of the longitudinal motion is determined by the simple form [3, 19, 21],

(4) $$\mathrm{v}_{therm} = \sqrt{T / M_t}.$$

This is often referred to as M_t scaling. After estimating the breakup temperatures from RHIC with other means, one can use the measurement of R_{long} to determine the mean emission time. This well complements the comparison of R_{out} to R_{side} which provides insight into the variance of emission times.

Thus, a measure of $g(\mathrm{v},\mathbf{r})$ can be used to determine both spatial and temporal information about the source. The ability to extract $g(\mathrm{v},\mathbf{r})$ from correlation measurements hinges on the ability to invert the expression,

(5) $$C(\mathrm{v},\mathbf{q}) = \int d^3r g(\mathrm{v},\mathbf{r}) \left|\psi(\mathbf{q},\mathbf{r})\right|^2$$

where $\psi(\mathbf{q},\mathbf{r})$ is the relative wave function of two particles with asymptotic relative momentum q, and v is the velocity of the two-particle center of mass, which will always be assumed to be zero by a fortuitous choice of reference frame. For identical spinless bosons, the relative wave function is particularly simple to invert, $|\psi(\mathbf{q},\mathbf{r})|^2 = 1 + \cos 2q\cdot r$. One can then perform a Fourier transform and retrieve $g(\mathrm{v},\mathbf{r})$. It has become standard procedure for experimentalists to divide $\pi^+\pi^+$ and $\pi^-\pi^-$ correlation functions by a Coulomb correction factor so that the resulting object can be treated as if the pions were never charged and g can be found by a Fourier transform.

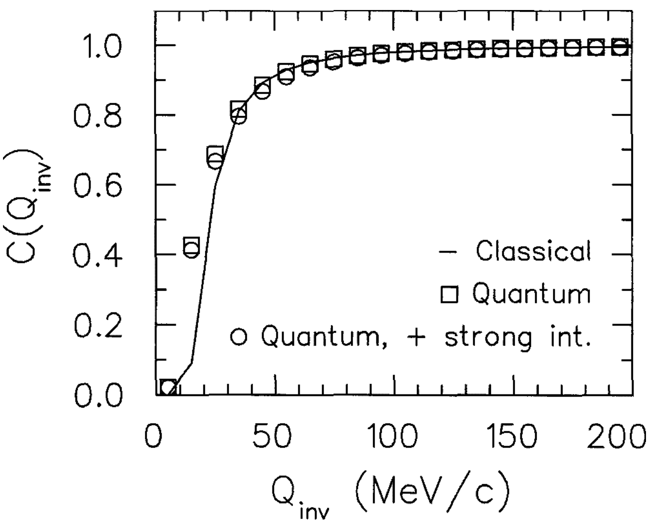

Fig. 1. pK^+ correlations are shown for a Gaussian source ($R_{long} = R_{side} = 4$ fm, $R_{out} = 8$ fm). The classical approximation well explains Coulomb correlations at large relative momentum. The strong interaction only moderately affects the correlation function.

Once the inversion has been identified as a Fourier transform it is especially easy to relate $g(\mathbf{r})$ and $C(\mathbf{q})$ for Gaussian shapes.

(6) if

$$g(\mathbf{r}) = \frac{1}{(4\pi)^{3/2} R_{out}R_{side}R_{long}} \exp - \left\{ \frac{r_{out}^2}{4R_{out}^2} + \frac{r_{side}^2}{4R_{side}^2} + \frac{r_{long}^2}{4R_{long}^2} \right\}$$

$$C(\mathbf{q}) = 1 + \exp\left\{-4q_{out}^2R_{out}^2 - 4q_{side}^2R_{side}^2 - 4q_{long}^2R_{long}^2\right\}$$

where q is the momentum of one particle in the pair frame.

Unfortunately, it is not so simple to relate $g(\mathbf{r})$ to $C(\mathbf{q})$ for pairs where the interaction is more complicated. Even the simple Coulomb interaction leads to an opaque form for the wave function to be inserted into Eq. (5). Figure 1 shows correlation functions for the pK^+ interaction calculated with Coulomb interactions assuming a Gaussian source of $R_{out} = 8$ fm, $R_{side} = R_{long} = 4$ fm. Results are also displayed for the corresponding classical expression [13] where,

(7)

$$\left|\psi(\mathbf{q},\mathbf{r})\right|^2 \to \frac{d^3q_o}{d^3q} = \frac{1 + \cos\theta_{qr} - \eta/(qr)}{\sqrt{\left(1+\cos\theta_{qr}\right)^2 - 2\left(1+\cos\theta_{qr}\right)\eta/(qr)}} \cdot \Theta\left(1 + \cos\theta_{qr} - 2\eta/(qr)\right)$$

where θ_{qr} is the angle between q and r. The classical and quantum results agree well when $qR >> 1$, or for $q >$ 50 MeV/c in heavy ion collisions. As the classical expression is more physically transparent, one can gain a clearer insight into the sensitivity of the correlation function to the size and shape from the classical expression. First, if one averages over all directions of q, one can see that the classical description has a simple form at large q,

$$\frac{d_0^2 dq_o}{q^2 dq} = \sqrt{1-\frac{2\eta}{qr}} \approx 1-\frac{\eta}{qr} \tag{8}$$

where $\eta \equiv \mu e^2/q$ with μ referring to the reduced mass. Thus, the correlation behaves as $(\mu e^2/q^2)<1/4>$ for large q.

The sensitivity of the correlation function to the shape can be seen by plotting the correlation as a function of the direction of q relative to the outwards axis. This is shown in Fig. 2. Again, the classical and quantum results agree well for larger relative momentum. At small relative momentum, the quantum calculation shows little sensitivity to the direction. At large relative momentum, the shape continues to scale as $1/q^2$ which allows one to use large bins in q. Since the interaction is repulsive it is not surprising that the correlation stays negative for all directions of q. However, one might be surprised at the strong sensitivity to the direction. Careful consideration of Eq. (7) shows that the classical correlation falls deeper in the $\cos\theta = \pm 1$ direction than the $\cos\theta = 0$ direction by a factor of R^2_{out}/R^2_{side}. Since the origins of the particles are more likely to be in direction $\cos\theta_r = \pm 1$, the particles traveling directly toward the deflecting charge will be directed away from the $\cos\theta = \pm 1$ directions by the repulsive Coulomb force.

Strong interactions also distort wave functions and thus potentially provide the means to extract size and shape information. For distances beyond the scale of the strong interaction, the wave functions are determined by phase shifts.

$$\begin{cases} \psi(\mathbf{q},\mathbf{r}) = \psi_0(\mathbf{q},\mathbf{r}) + \sum_l \sqrt{4\pi(2l+1)}\frac{i^l}{2qr}e^{-i\sigma_l} \\ \qquad \cdot\left(F_l(\eta,qr) - iG_t(\eta,gr)\right)\left(e^{-2i\sigma_l}-1\right)Y_{l,m=0} \\ \sigma_l \equiv \arg\left(\Gamma(1+l+i\eta)\right) \end{cases} \tag{9}$$

However, inside the range of the strong interaction the wave function ψ is varied in ways that depend on the exact form of the potential. In fact, since the wave function is only a sensible object for two well defined particles, it is not even a physical object for small distances when scattering proceeds through a resonance. Fortunately, the form of the wave function is not important for distances much less than characteristic scales of the source. Only the integral integral of $|\psi(q,r)|^2$ matters for the range, $r < \varepsilon$, and one can safely assume that the alteration of the wave function is described by an effective constant.

$$|\psi(q,r<\varepsilon)|^2 = |\psi_0(q,r)|^2 + W(\varepsilon,q) \tag{10}$$

where ψ_0 is the Coulomb wave and W is independent of r. Fortunately, the integral of $|\psi|^2$ is related to the density of states and can be expressed in terms of the derivatives of the phase shifts [12].

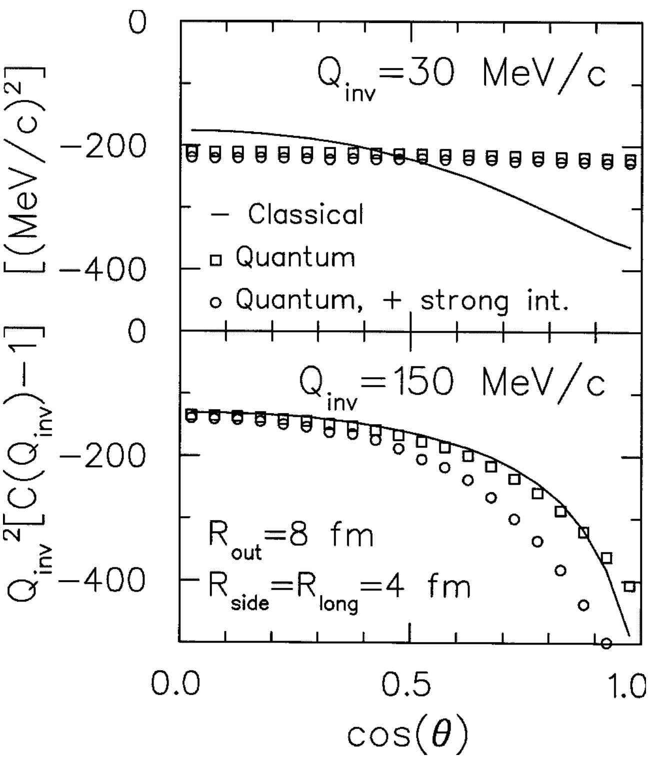

Fig. 2. pK^+ correlations are shown as a function of the angle of the relative momentum relative to the outwards direction for the Gaussian source ($R_{long} = R_{side} = 4$ fm, $R_{out} = 8$ fm). The classical approximation becomes reasonable for large Q_{inv} where the ratio of the suppression at $\cos\theta = 1$ to the suppression at $\cos\theta = 0$ approaches $(R_{out}/R_{side})^2$.

$$\begin{cases} \Delta\frac{dN}{dq} = \frac{4\pi q^2}{(2\pi)^3}\int d^3r\left(|\psi(\mathbf{q},\mathbf{r})|^2 - |\psi_o(\mathbf{q},\mathbf{r})|^2\right) \\ \quad = \sum\frac{(2l+1)}{\pi}\frac{d\delta_l}{dq} = \frac{2q^2\varepsilon^3}{3\pi}W(\varepsilon,q) \\ \quad + 2\sum\frac{(2l+1)}{\pi}\int_\varepsilon^\infty dr\left(|\varphi_l(\eta,qr)|^2 - |F_l(\eta,qr)|^2\right) \\ \phi_l = F_l + \frac{1}{2}\left(e^{-2i\delta_l}-1\right)\left(F_l - iG_l\right). \end{cases} \tag{11}$$

Thus, W can be expressed in terms of derivatives of the phase shifts and integrals of the wave function over a range in which the wave function is known. Since these integrals can be performed analytically, W can be expressed in closed form [22].

Examples of the effects of the strong interaction are shown in Figs. 1 and 2 for pK^+correlations and for $p\pi^+$ correlations in Fig. 3. The strong interaction has little effect on pK^+correlations since phase shifts vary little. Not surprisingly, the strong interaction provides a noticeable correlation for $p\pi^+$ pairs with the relative momentum chosen to be near the peak of the Δ resonance. The angular correlations for the $R_{out} = 8$ fm, $R_{side} = R_{long} = 4$ fm $p\pi^+$ source shown in Fig. 3 are positive for $\cos\theta$ near zero and become negative near $\cos\theta = \pm 1$. The angular sensitivity has two sources.

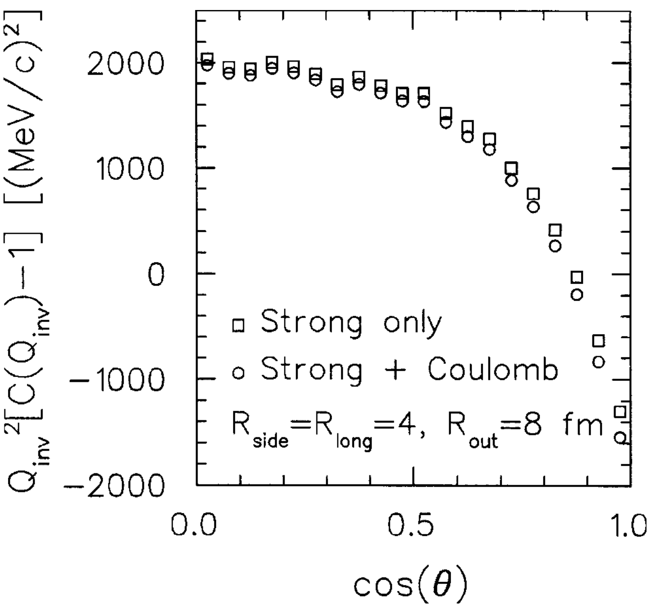

Fig. 3. pK^+ angular correlations for a Gaussian source (R_{out} = R_{side} = 4 fm, R_{long} = 8 fm) with Q_{inv} = 450 MeV/c. At this Q_{inv} the correlation is dominated by the Δ^{++} resonance. The behavior at $\cos\theta = 1$ is due to interference between the scattered partial wave and the initial plane wave.

Squaring the second term in Eq. (9) provides a contribution proportional to the square of the scattering amplitude, $|f(\Omega)|^2$. This contribution has the same angular behavior as a scattered plane wave. For the $p\pi$ example, this would have led to maxima for $\cos\theta \sim \pm 1$ rather than the minima which are seen in Fig. 3. The second source of angular dependence stems from the interference between the initial plane wave and the partial wave corrections. This interference will be strongest in the direction $\cos\theta_{qr} = -1$ since the phases then share the same r dependence, e^{-iqr}. The source points in this direction are those from which the trajectories must pass directly over the origin. For $\cos\theta_{qr} = -1$, the wave function can be written as

$$(12)\quad \psi(q,r)\Big|_{\cos\theta_{qr=-1}} = e^{-iqr}\left(1+\sum(2l+1)e^{-i\delta_l}\sin\delta_l\frac{1}{2qr}+O1(qr)^2\right)$$

and one can see that the interference between the scattered and plane wave is strong in this direction. This diffractive behavior provides the leverage for extracting shape information from the correlation function.

Finally, I wish to make a connection of the analysis here to the Lednický analysis [7, 14, 15, 23, 27] which compares correlations for $\cos\theta > 0$ to those for $\cos\theta < 0$ for non-identical particles. The Lednický analysis is sensitive to the dipole moment of the distribution, i.e., the offset of one particle distribution to that of another type of particle with the same velocity. By analyzing the correlation as a function of $\cos\theta$, as is shown here, one can gain insight into the higher moments. For instance, the five quadrupole terms represented by $Y_{l=2,m}$, along with the monopole moment represent the typical variables used to describe an elliptic anisotropy. Geometrically, these six variables correspond to the three axes of the ellipse along with the three Euler angles that describe the orientation of the ellipse. In terms of Gaussian parameters, these six variables would translate into the three Gaussian radii and the three cross terms [9]. These are precisely the terms that provide insight into the space-time nature of the source. In principal, much more information is available, and one could consider using these correlations to image the source and provide higher angular moments as well as a more precise radial (non-Gaussian) form [5, 20, 26]. Given the importance of HBT measurements from identical-pion and identical-kaon correlations, the experimental community should give the highest priority toward investigating the complementary information provided by non-identical correlations regarding source size, shape and lifetime.

This work was supported by the U.S. Department of Energy, Grant No DE-FG02-03ER41259.

References

1. Adcox K, Adler SS, Ajitanand NN *et al.* (for the PHENIX Collaboration) (2003) Transverse mass dependence of two-pion correlations in Au+Au collisions at %s(NN)**(1/2) = 130 GeV. Phys Rev Lett 88:192302
2. Adler C, Ahammed Z, Allgower C *et al.* (for the STAR Collaboration) (2001) Pion interferometry of s(NN)**(1/2) = 130 GeV Au+Au collisions at RHIC. Phys Rev Lett 87:082301
3. Akkelin SV, Borisova MS, Sinyukov YuM (2004) Influence of resonances on pion spectra and interferometry volume in relativistic heavy ion collisions. Nukleonika 49;S2:s115–s118
4. Baker M (for the PHOBOS Collaboration) (2003) Global observations from PHOBOS. (nucl-ex/0212009)
5. Brown DA, Danielewicz P (2001) Observing non-Gaussian sources in heavy-ion reactions. Phys Rev C 64:014902
6. Csanád M, Csörgő T, Lörstad B, Ster A (2004) A hint at quark deconfinement in 200 GeV Au+Au data at RHIC. Nukleonika 49;S2:s49–s55
7. Gelderloos CJ, Alexander JM, Ajitanad NN *et al.* (1995) Time relationships between direct particle emission and fragmentation: a probe for nuclear expansion prior to fragment freeze-out. Phys Rev Lett 75:3082–3085
8. Gyulassy M, Rischke D (1996) The time-delay signature of quark-gluon plasma formation in relativistic nuclear collisions. Nucl Phys A 608:479–512
9. Heinz U, Hummel A, Lisa MA, Wiedemann UA (2002) Symmetry constraints for the emission angle dependence of Hanbury-Brown-Twiss radii. Phys Rev C 66:044903
10. Heinz U, Jacak B (1999) Two-particle correlations in relativistic heavy-ion collisions. Annu Rev Nucl Part Sci 49:529–579
11. Humanic TJ (2003) Comparison of hadronic rescattering calculations of elliptic flow and HBT with measurements from RHIC. Nucl Phys A 715:641–644
12. Jennings B, Boal D, Shillcock J (1986) Two-particle correlation functions in the thermal model and nuclear interferometry descriptions. Phys Rev C 33:1303–1306
13. Kim Y, de Souza R, Gelbke C, Gong W, Pratt S (1992) Final-state Coulomb interactions for intermediate-mass fragment emission. Phys Rev C 45:387–395
14. Kotte R, Barz HW, Neubert W *et al.* (1999) On the space-time difference of proton and composite particle emission in central heavy-ion reactions at 400 AmeV. Eur Phys J A 6:185–195
15. Lednický R, Lyuboshitz VL, Erazmus B, Nouais D (1996) How to measure which sort of particles was emitted earlier and which later. Phys Lett B 373:30–34

16. Lin Z, Ko CM, Pal S (2002) Partonic effects on pion interferometry at the relativistic heavy-ion collider. Phys Rev Lett 89:152301
17. Lisa MA (2004) Azimuthally-sensitive interferometry and the source lifetime at RHIC. Nukleonika 49;S2:s71–s76
18. López Noriega M (2004) Pion interferometry in Au+Au collisions at s(NN)**(1/2) = 200 GeV. Nukleonika 49;S2:s67–s70
19. Makhlin A, Sinyukov YuM (1988) The hydrodynamics of hadron matter under a pion interferometric microscope. Z Phys C 39:69–76
20. Panitkin SY, Ajitanand NN, Alexander JM *et al.* (for the E895 Collaboration) (2001) Model-independent source imaging using two-pion correlations in 2 to 8 AGeV Au+Au collisions. Phys Rev Lett 87:112304
21. Pratt S (1986) Pion interferometry of quark-gluon plasma. Phys Rev D 33:1314–1327
22. Pratt S, Petriconi S (2003) Alternative size and lifetime measurements for high-energy heavy-ion collisions. Phys Rev C 68:054901
23. Shin Y, Ahner W, Barth R (KaoS Collaboration) (1998) Enhanced out-of-plane emission of K+ mesons observed in Au+Au collisions at 1 AGeV. Phys Rev Lett 81:1576–1579
24. Soff S, Bass S, Dumitru A (2001) Pion interferometry at RHIC: Probing a thermalized quark-gluon plasma? Phys Rev Lett 86:3981–3984
25. Teaney D, Lauret J, Shuryak E (2001) A hydrodynamic description of heavy ion collisions at the SPS and RHIC. (nucl-th/0110037)
26. Verde G, Danielewicz P, Lynch W, Brown D, Gelbke C, Tsang M (2002) Imaging sources with fast and slow emission components. Phys Rev C 65:054609
27. Voloshin S, Lednický R, Panitkin S (1997) Relative space-time asymmetries in pion and nucleon production in noncentral nucleus-nucleus collisions at high energies. Phys Rev Lett 79:4766–4769